**Revised figures and tables for O'Brien et al. for *Phil Trans Roy Soc* special issue**

**Figure 1**: Population genetic models of local adaptation highlight how interactions between adaptive potential (genetic variance in fitness) and genetic load (population mean fitness), both of which are increased by gene flow, determine when and where populations can track changing optima in space.
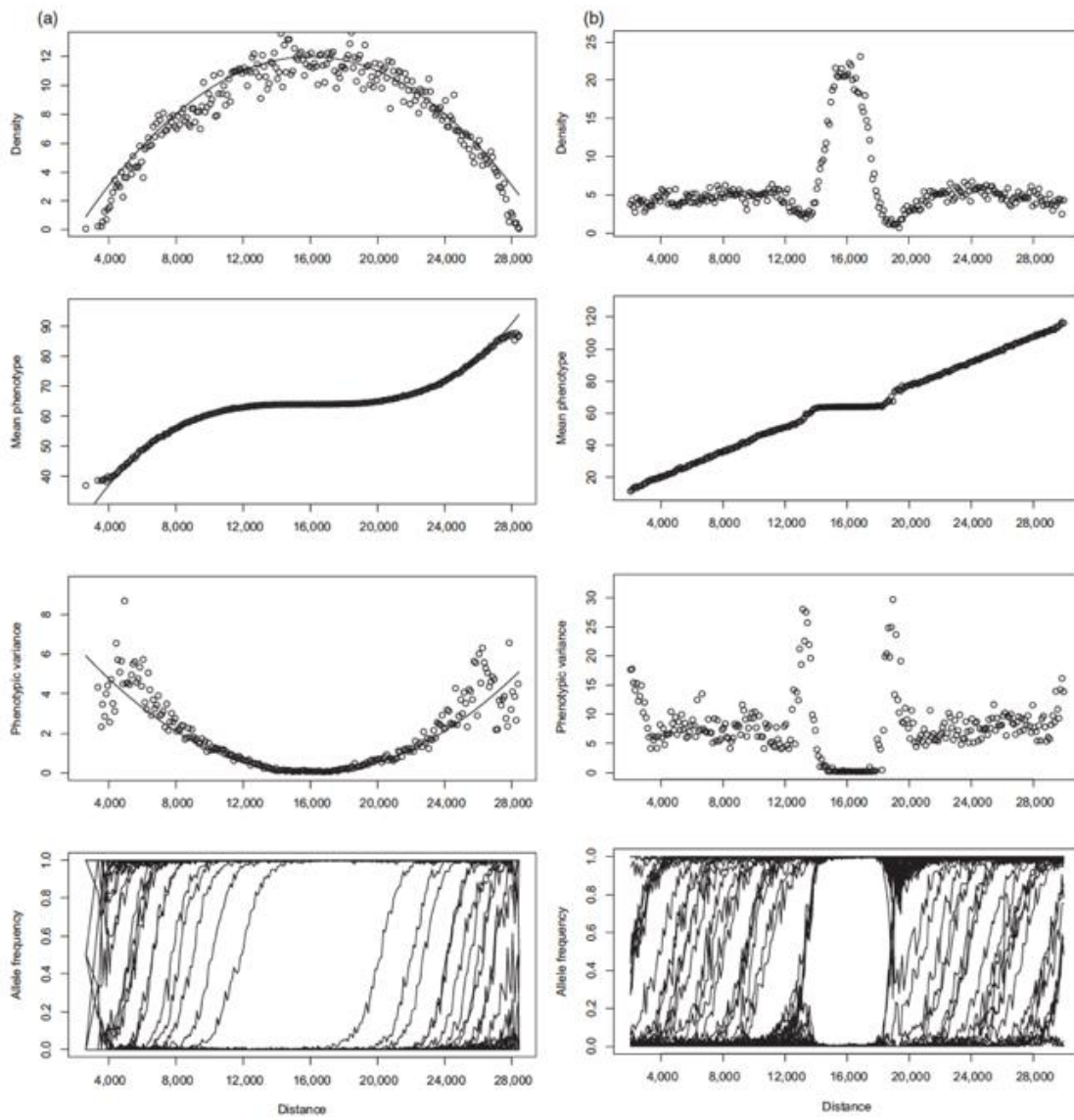
*(a) Limits to adaptation along a steepening (left panel) and non-linear gradient (right panel).* Genetic variance facilitates adaptation until a critical threshold for a given population size and maximum rate of growth, where genetic load prevents an effective response to selection relative to genetic drift. Regions of increased load can be associated with local increases in asymmetric gene flow and/or gradient steepness, or changes in phenotype where the frequencies of many alleles need to change in the same position (bottom panels). Note how local reductions in density correlate with regions of increased phenotypic variance. These finite range edges occur because concomitant increases in adaptive potential are insufficient to track the local optimum, as reflected by a mismatch between the optimal (solid line) and the actual population means (open circles). (from Bridle et al. (2019) *Evolutionary Applications*).

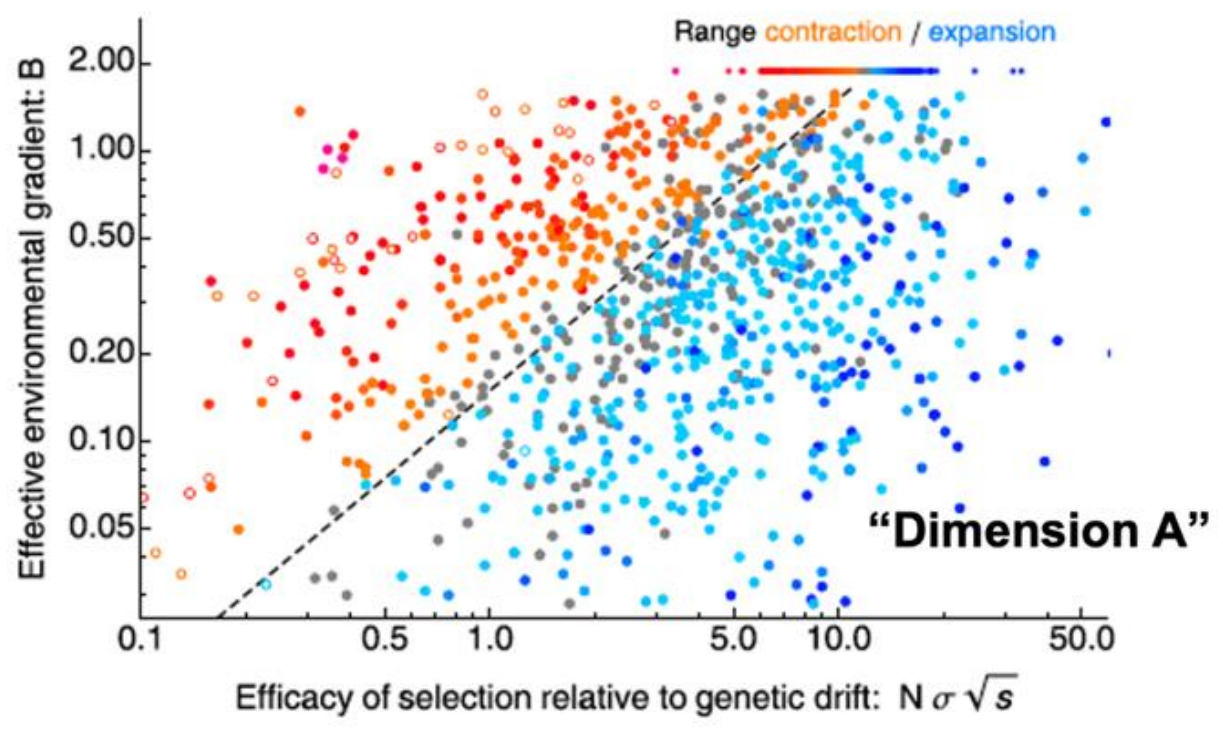(b): *A framework for predicting when and where local adaptation fails along a one-dimensional ecological gradient.* Dimension [A] and Dimension [B] determine the critical threshold for niche expansion versus contraction along spatially varying gradients. Dimension [A] relates to the ability for selection to overcome drift, based on the standard deviation of dispersal per generation along the gradient ($\sigma$); the sqrt of the strength of selection per locus (s); and the population size (N). Dimension [B] summarises the steepness of the environmental gradient, which includes the amount of mean dispersal along it, so scaling the gradient in terms of how ecological variation is experienced by alleles across generations and genotypes. The critical threshold is shown as a dotted line, and the rate of population expansion or contraction denoted by blue and red dots respectively. Open dots denote populations that fragment along their range; grey dots parameter values where the outcome is unclear (Reprinted from Polechová and Barton (2015) with minor modifications. Original image © 2015 National Academy of Sciences).

Fig 1a

(Fig 1b)

## "Dimension B"

## Box 1: A framework for predicting limits to adaptation

**[DIMENSION A] "Efficacy of selection"**

*Affecting the power of selection vs genetic drift; and the demographic cost (load) vs benefit of genetic variation*

1. Reproductive output at optimum ($R_{max}$)
2. Strength of selection (cost of being away from optimum)
3. How much genetic variation in fitness?
4. How does gene flow affect variance in fitness (genomic architecture + recombination + plasticity)?
5. How many traits/alleles need to change to match the optimum (How many genomic routes? How strong are ecological trade offs?)

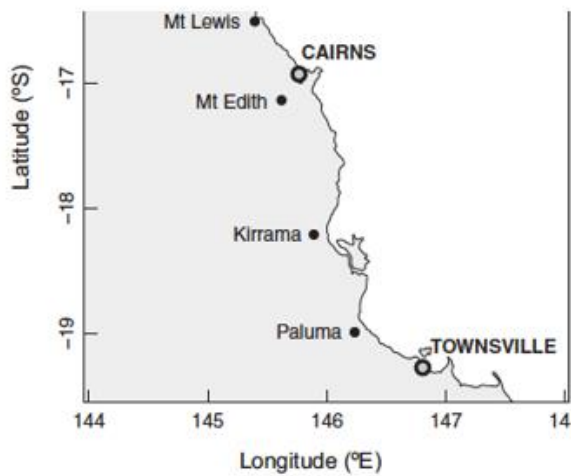**[DIMENSION B] "Effective environmental gradient"**

*Affecting the environmental gradient from allele/genotype's perspective*

6. How steep is the gradient (and how much dispersal along it?)
7. How patchy or smooth is the gradient in space or time?
8. How predictable and how directional is selection
9. In how many different ways is the [genetic and ecological] environment changing?

**Box 1**: A framework for predicting niche expansion vs contraction, highlighting key parameter values that may affect where given populations in space or time lie along the Dimensions [A] and [B] in Polechová and Barton (2015; Fig 1b), or create departures from these expectations, particularly when temporal as well as spatial change in trait optima are included (see main text). Lessons for how many of these factors vary in real populations and may affect maximum rates of evolution are summarised in the text, largely from attempts to test such theory in populations of rainforest *Drosophila* and the UK *Brown Argus* butterfly.

**Figure 2:** (a) Location of elevational transects studied in Queensland, and photos showing a typical elevational transition, and (insert) *D. birchii* and *D. bunnanda* females; (b) left: Mean cold tolerance (time to recover from chill coma) of *D. birchii* isofemale lines, and right: *D. birchii* field density (black squares) and mean daily temperature (open circles) at sites along the Kirrama elevation gradient sampled in 2004 (top) and 2010 (bottom). For cold tolerance, black squares represent sites where ≥5 lines were used to calculate the mean and white squares where <5 lines were available. Error bars are standard errors among lines. For field density, error bars are standard errors between sampling days. Data from 2010 in (b) are presented here for the first time; data from 2004 are from Bridle et al. (2009).
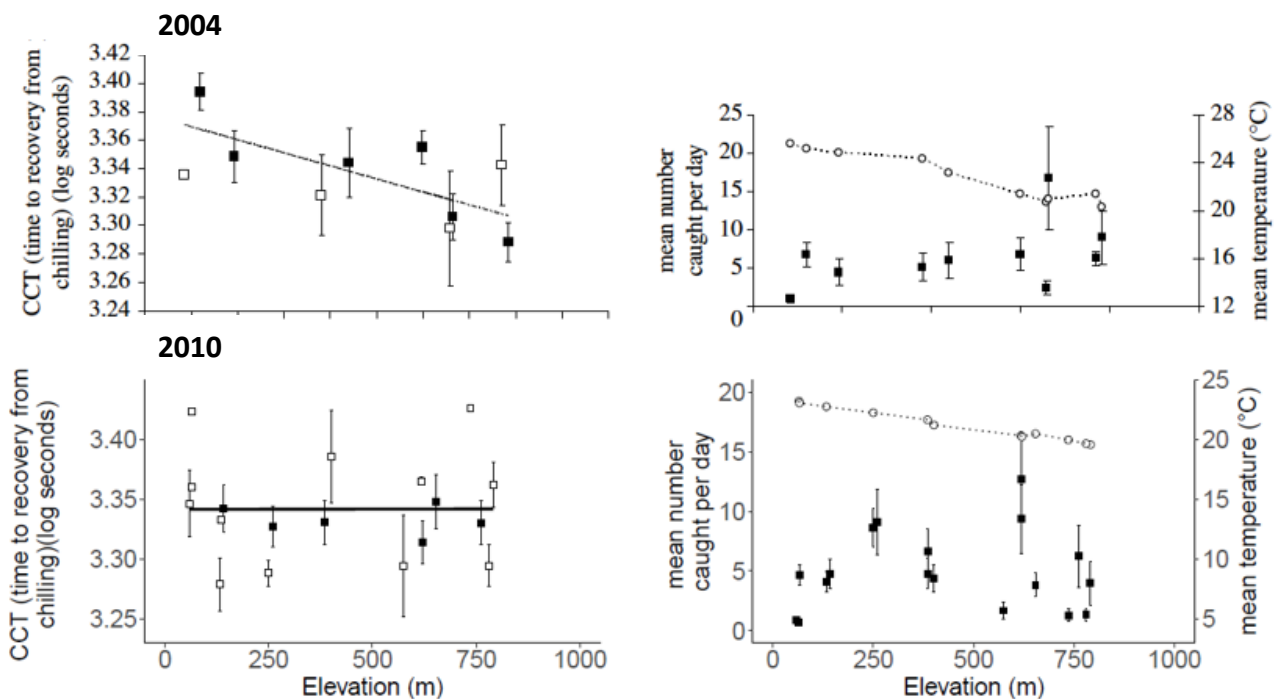
(a)



(b)

**Figure 3.** Productivity of *D. birchii* isofemale lines collected in 2012 from low and high elevation sites at Mt Edith (left) and Paluma (right) when reared in the laboratory at 25 ˚C. Error bars are standard errors among lines. High elevation lines had significantly higher productivity than low elevation lines from both gradients. This variation in lab productivity among source populations is not observed in field transplant cages (Figure from O'Brien et al 2017, SI).
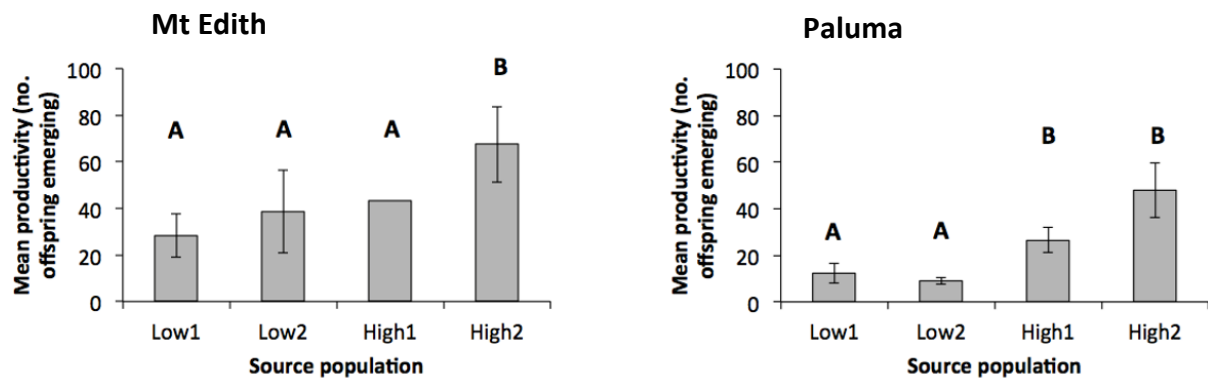
**Figure 4.** Field density, trait means, variances and genetic correlations for *D. birchii* sampled from sites along three elevation gradients (Mt Lewis, Mt Edith and Paluma) in 2011. Data here are presented for the first time – see SI for methods. **(a)** Top row: *D. birchii* field density (black squares) and mean daily temperature (open circles).  Middle row: mean cold tolerance (measured as offspring produced following a cold shock). Bottom row: mean wing size; **(b)** Heritability of cold tolerance and wing size and genetic correlations between these traits.  For field density, error bars are standard errors between sampling days.  For trait means, heritabilities and genetic correlations, error bars are the 95% highest posterior density intervals of the relevant parameter estimates from MCMCglmm models.
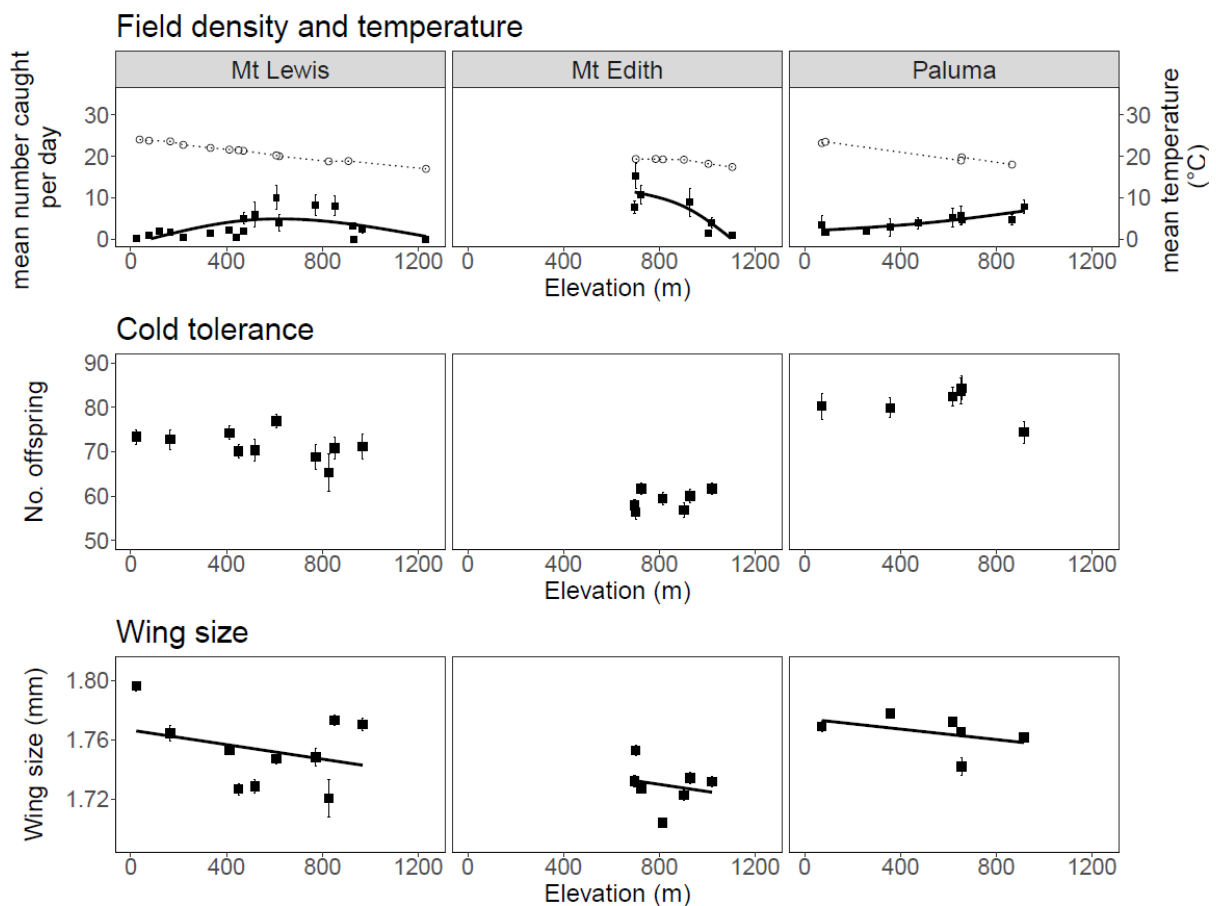
Fig 4 (a)

Fig 4 (b)

Heritability: Cold tolerance



Heritability: Wing size



Genetic correlation: Cold tolerance & Wing size